Biochemistry
Article
Cite This: Biochemistry 2018, 57, 839−851
pubs.acs.org/biochemistry

# A Negative Allosteric Modulator of WNT Receptor Frizzled 4 Switches into an Allosteric Agonist

Gennaro Riccio,[†] Sara Bottone,[†] Giuseppe La Regina,[‡] Nadia Badolati,[†] Sara Passacantilli,[‡] Giovanni Battista Rossi,[§] Antonella Accardo,[†] Monica Dentice,[∥] Romano Silvestri,[‡] Ettore Novellino,*[,†] and Mariano Stornaiuolo*[,†]

[†]Department of Pharmacy, University of Naples Federico II, Naples, Italy

[‡]Istituto Pasteur-Fondazione Cenci Bolognetti, Dipartimento di Chimica e Tecnologie del Farmaco, Sapienza University of Rome, Rome, Italy

[§]Gastroenterology and gastrointestinal endoscopy unit, Istituto Nazionale Tumori-IRCCS-Fondazione G. Pascale, Naples, Italy

[∥]Department of Clinical Medicine and Surgery, University of Naples Federico II, Naples, Italy

Supporting Information

**ABSTRACT:** The WNT pathway interconnects a network of signaling events involved in a huge plethora of cellular processes, from organogenesis to tissue homeostasis. Despite its importance, the exiguity of organic drugs directly targeting the members of the Frizzled family of WNT receptors has hampered progress across the whole spectrum of biological fields in which the signaling is involved. We here present FzM1.8, a small molecule acting as an allosteric agonist of Frizzled receptor FZD4. FzM1.8 derives from FzM1, a negative allosteric modulator of the receptor. Replacement of FzM1 thiophene with a carboxylic moiety induces a molecular switch in the lead and transforms the molecule into an activator of WNT signaling. We here show that, in the absence of any WNT ligand, FzM1.8 binds to FZD4, promotes recruitment of heterotrimeric G proteins, and biases WNT signaling toward a noncanonical route that involves PI3K. Finally, in colon cancer cells, we prove that the FZD4/PI3K axis elicited by FzM1.8 preserves stemness and promotes proliferation of undifferentiated cells.

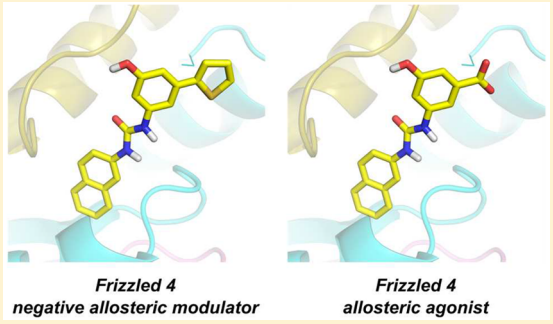


The 10 members of the human Frizzled (FZD) receptor family respond to the extracellular ligands of the wingless/int1 (WNT) family of lipo-glycoproteins. They control differentiation, organogenesis, and patterning in the developing embryo and somatic stem cell maintenance, tissue homeostasis, and regeneration in adult organisms. Dysregulation of WNT signaling leads to cancer stem cell genesis and tumor proliferation and has been linked to many types of malignancies.[1−4]

Despite their involvement in many cellular processes, several aspects of the mechanisms underpinning the activity of FZDs are still obscure.[5] The complexity arises from the multitude of WNT/FZD combinations (19 WNT ligands for 10 FZDs) and is further augmented by the many interconnected signaling networks each pair can activate.[6] Depending on the cascade, WNT/FZD signaling may involve heterotrimeric G proteins,[7,8] the cytosolic proteins Dishevelled (DVL),[9] or small GTPases.[10] The existence of FZDs as oligomers[11] and the participation of coreceptors like low-density lipoprotein receptor-related proteins 5 and 6 (LRP5/6) or receptor TK-like orphan receptor (ROR1/2)[12] influence downstream signaling and create additional levels of complexity.

In the "canonical" $\beta$-catenin-dependent pathway, binding of WNT to FZDs recruits DVL at the plasma membrane (PM). The WNT−FZD−DVL complex inactivates the APC destruction complex (formed by GSK3$\beta$, Axin, and Adenomatous Polyposis Coli)[13] and leads to the intracellular accumulation and nuclear translocation of $\beta$-catenin. In the nucleus, $\beta$-catenin regulates TCF/LEF-dependent transcription of WNT/$\beta$-catenin target genes like *cyclin D1*, *c-myc*, and *lgr5*.

Progress in the WNT field has been always hampered by the enormous difficulties associated with obtaining recombinant, pure, and biologically active WNTs and with the exiguity of pharmacological compounds that can directly target FZDs. In this complex scenario, small organic molecules acting as orthosteric or allosteric agonists for FZDs would represent essential biotools either for basic science or for pharmaceutical application. Allosteric ligands offer more options than orthosteric ones. They may (i) present intrinsic agonist activity (allosteric agonists), (ii) potentiate endogenous orthosteric agonists [positive allosteric modulators (PAMs)], (iii) possess

**Received:** October 28, 2017
**Revised:** December 20, 2017
**Published:** January 2, 2018





DOI: 10.1021/acs.biochem.7b01087
Biochemistry 2018, 57, 839−851

both properties mentioned above (ago-PAM), or (iv) inhibit activation of the receptor [negative allosteric modulators (NAMs)]. In addition, allosteric modulators may introduce a "bias" that alters either the affinity of their cognate receptor for a specific agonist (ligand bias) or its propensity to activate a specific downstream signaling pathway (signal bias).[14]

We have recently identified FzM1, a NAM of FZD4 (a FZD family member).[15] FzM1 binds to an allosteric binding site located in intracellular loop 3 (ICL3) of FZD4 and alters the conformation of the receptor, ultimately inhibiting the WNT/$\beta$-catenin cascade.

Allosteric modulators exhibit fundamental changes in their modes of efficacy (known as a "molecular switch") when minor structural changes are made to their scaffold.[16,17] The same allosteric modulator can be thus converted into ago-PAMs, PAMs, and NAMs.[14,18] Here we show that the replacement of the FzM1 thiophene with a carboxylic moiety induces a molecular switch and generates, to the best of our knowledge, the first described allosteric agonist of FZD4, here termed FzM1.8.

FzM1.8 potentiates the $\beta$-catenin pathway in the absence of any WNT ligand. Upon binding, FzM1.8 biases FZD4 signaling toward a FZD4/PI3K axis that culminates into transactivation of $\beta$-catenin/TCF activity by the histone acetyltransferase CBP/p300. The binding site, mechanism of action, and competition with endogenous agonists are described here together with the physiological role of the FZD4/PI3K signaling axis.

## MATERIALS AND EXPERIMENTAL PROCEDURES

**Cell Cultures.** HEK293, CaCo-2, HuH7.5, and U87MG cells were grown in DMEM (41965-039, GIBCO, Thermo Fisher Scientific) supplemented with 10% FBS (10270, GIBCO), Glutamax (35050-061, GIBCO), and Pen/Strep (15070-063, GIBCO). HEK293 transfection was performed using PEI.[15] CaCo-2 and HuH7.5 transfection was performed using Lipofectamine (Invitrogen) following the manufacturer's instructions. Cell viability was measured with Trypan blue and propidium iodide. The percentage of apoptotic cells was measured with Mitotracker red (Life Technologies) following the manufacturer's instructions.

**DNA.** All DNA constructs were synthesized at GenScript. The cDNAs encoding N-terminally HA-tagged FZD4wt (HA-FZD4-wt) and mutants HA-FZD4-T425A and HA-FZD4-T425D were all cloned in expression vector pCDNA3.1 (Invitrogen). For the reporter construct WRE-GFP-wt, eight repeats of the optimized TCF/LEF binding sequence (5′-AGATCAAAGGGG-3′) (interspersed with the 5′-GTA-3′ triplet) were positioned upstream from a minimal TATA box promoter (5′-tagagggtatataatggaagctcgaattccag-3′) and a KOZAC region (5′-cttggcattccggtactgttggtaaaaagcttggcattccgg-tactgttggtaaagccacc-3′). The sequence was cloned in vector pCDNA 3.1 (+) GFP between the restriction sites for NruI and HindIII. This replacement substitutes for the CMV promoter of the original vector with the TCF/LEF responsive sequences. The correctness of the sequences was verified by DNA sequencing. Control reporter construct WRE-GFP-mut was obtained by mutagenesis of WRE-GFP-wt and presents the eight repeats of the TCF/LEF binding sequence mutated to 5′-AGGCCAAAGGGG-3′. A reporter construct (cmv-GFP) presenting GFP under the control of the CMV promoter was used as a control. The plasmid necessary for the expression of human AKT mutant AKT-K179M was kindly provided by G. Condorelli (Naples, Italy).

**TCF/LEF Activity Measurement Using the WRE-GFP Constructs.** HEK293 cells were seeded ($5 \times 10^3$ per well) in 96-well black Optyplates (PerkinElmer). After 24 h, cells were co-transfected with both WRE-GFP-wt (or where indicated WRE-GFP-mut) and HA-FZD4-wt. Transfection mixtures were prepared as follows. In each well, 0.25 $\mu$g of PEI (pH 7.0) was supplemented with 0.08 $\mu$g of DNA (both diluted in 4 $\mu$L of DMEM). The mixture was incubated at room temperature for 30 min, diluted in culture medium, and added to the cells. Twenty-four hours after transfection, the medium was replaced and cells were incubated with FzM1 and FzM1.8 at the indicated concentrations for the indicated times. When reported, cells were supplemented with either CKI 7 dihydrochloride (5 $\mu$M), NFAT inhibitor (10 $\mu$M), bisindolylmaleimide II (7.5 $\mu$M), Ly294002 (10 $\mu$M), Suramin hexasodium salt (10 $\mu$M), Gallein (10 $\mu$M), or I-CBP 112 (7.5 $\mu$M). At the end of the incubations, cells were fixed in 3.7% formaldehyde in PBS (pH 7.4) for 30 min. Formaldehyde was quenched by incubating the cells for 30 min in 0.1 M glycine in 1× PBS. The activity of the compounds was evaluated by measuring GFP expression.

**WNT5A-Conditioned Medium.** Human glioblastoma U87MG cells were the source of WNT5A-conditioned medium.[39] Confluent 6 cm plates of U87MG cells were incubated for 3 days in DMEM, 10% FBS, and Glutamax in the absence of antibiotics. Conditioned medium was thus collected and stored at −20 °C. Cells were then rinsed with fresh medium and cultivated for an additional 3 days. The conditioned medium obtained after the second incubation was pooled with the first portion. The pooled conditioned medium was used to stimulate TCF/LEF activity in HEK293 cells.

**Antibodies.** The following antibodies were used. The mouse monoclonal anti-HA peptide (HA-7) (H3663, Sigma-Aldrich) was used at a 1/2000 dilution for both Western blotting (WB) and immunofluorescence (IF), while a 1/200 dilution was used for immunoprecipitation (IP). Mouse monoclonal anti-$\alpha$-tubulin (10D8, sc-53646, Santa Cruz Biotechnology, Santa Cruz, CA) (WB, 1/200), rabbit polyclonal anti-$\beta$-catenin (H-102, sc-7199, Santa Cruz Biotechnology) (WB, 1/1000), rabbit polyclonal anti-HA peptide (H6908, Sigma-Aldrich) (WB, 1/2000; IF, 1/500; IP, 1/500), rabbit anti-AKT (9272, Cell Signaling Technology, Danvers, MA) (WB, 1/1000), rabbit anti-phospho-AKT (Thr308) (D25E6, 13038, Cell Signaling Technology) (WB, 1/2000), rabbit anti-phospho-AKT (Ser473) (D9E, 4060, Cell Signaling Technology) (WB, 1/2000), goat anti-rabbit IgG (H&L) DyLight 594 conjugate (GtxRb-003-D594NHSX, ImmunoReagents, Inc., Raleigh, NC) (IF, 1/500), donkey anti-rabbit IgG (H&L) HRP conjugate (DkxRb-003-DHRPX, ImmunoReagents, Inc.) (WB, 1/4000), goat anti-mouse IgG (H&L) DyLight 594 conjugate (GtxMu-003-D594NHSX, ImmunoReagents, Inc.) (IF, 1/500), goat anti-mouse IgG (H&L) HRP conjugate (GtxMu-003-DHRPX ImmunoReagents, Inc.) (WB, 1/4000) were also used.

**Western Blotting.** Cells were lysed in 50 mM Hepes-KOH, 150 mM NaCl, and 1% Triton X-100, supplemented with protease inhibitors (Roche). Lysates were centrifuged at 14000 rpm for 30 min at 4 °C. The total amount of proteins in each lysate was measured using the Bradford assay. Before sodium dodecyl sulfate−polyacrylamide gel electrophoresis (SDS−


DOI: 10.1021/acs.biochem.7b01087
Biochemistry 2018, 57, 839−851

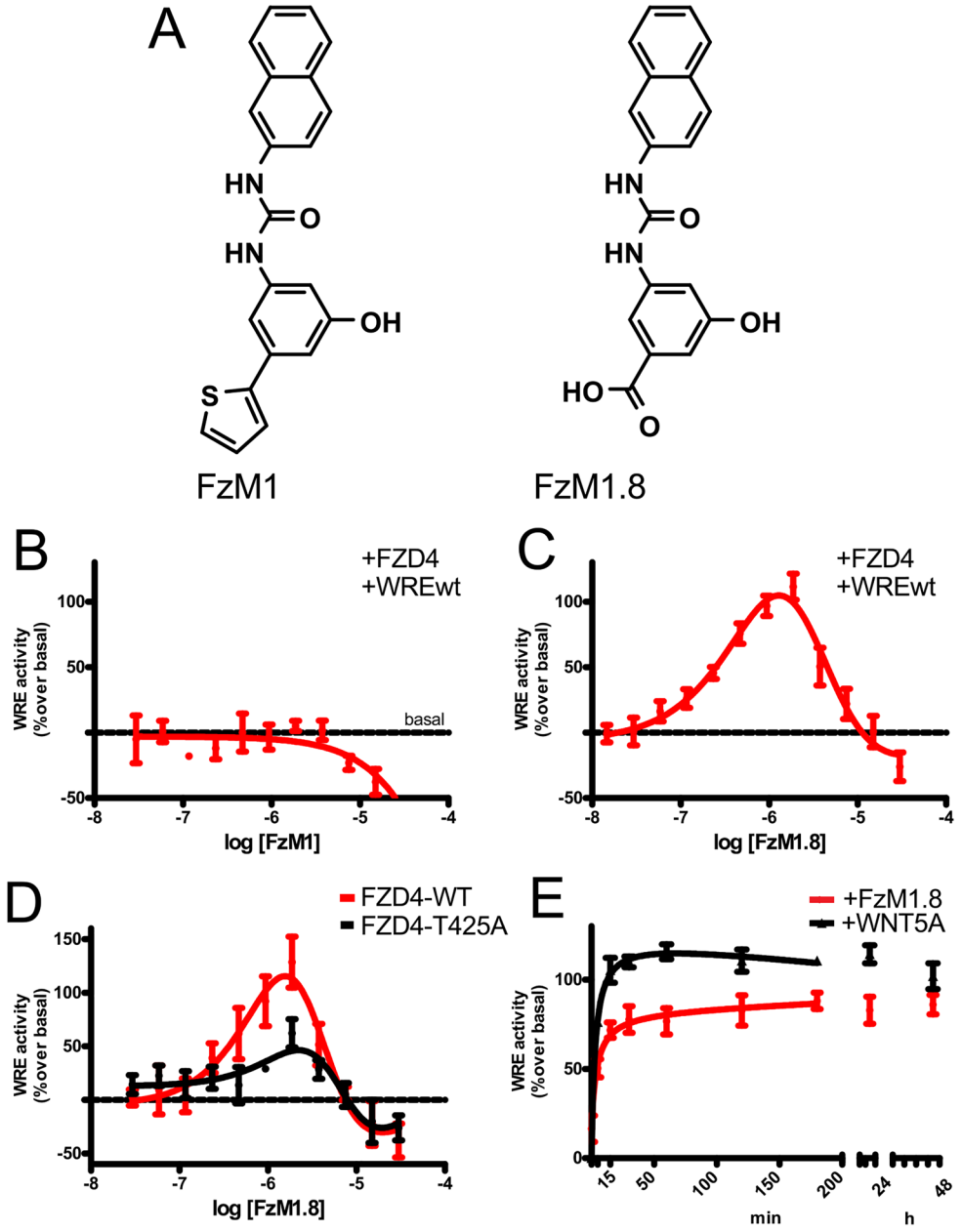


**Figure 1.** FzM1.8 is an allosteric agonist of FZD4 and activates the WNT/$\beta$-catenin pathway. (A) Chemical structures of FzM1 and FzM1.8. (B and C) Dose−response curves for FzM1 and FzM1.8 modulation, respectively, of the WNT/$\beta$-catenin pathway in HEK293 cells expressing FZD4-wt. Values indicate changes in WRE activity (expressed as the percentage of change over basal activity). (D) Dose−response curves for FzM1.8 modulation of WRE activity in HEK293 cells expressing FZD4wt (red) or FZD4-T425A (black). (E) Response elicited by incubating HEK293 cells (transiently expressing FZD4-wt) with FzM1.8 (2 $\mu$M, red) or WNT5A (conditioned medium, black) for the indicated period of time. Values are reported as means ± the standard error of the mean ($n$ = 5).

PAGE), each lysate was diluted in 20 mM Tris-HCl (pH 6.8), 50 mM DTT, 1% SDS, 5% glycerol, and bromophenol blue and then boiled for 10 min at 95 °C (for SDS analysis of FZD4, lysates were not boiled but incubated for 30 min at 37 °C). SDS−PAGE gels were run at 100 V (25 °C). For Western blotting analysis, proteins were transferred onto PVDF membranes (IB24001, Invitrogen, Thermo Fisher Scientific) using the iBlot 2 Gel Transfer Device (Invitrogen, Thermo Fisher Scientific). After the transfer, PVDF membranes were first incubated in a blocking solution (1× PBS, 5% nonfat dried milk) for 2 h at 25 °C and then incubated with primary and secondary antibodies supplemented with 0.3% nonfat dry milk. ECL reactions were performed as previously described.[15] The immunoreactive bands were detected by chemiluminescence and quantitated using ImageQuant (GE Healthcare, Little Chalfont, U.K.).

**Immunofluorescence.** Immunofluorescence was assessed as previously described.[15] Briefly, HEK293 cells seeded at a density of 5000 cells/well in a ViewPlate-96 Black, Optically Clear Bottom plate (6005182, PerkinElmer) were transfected with PEI as described above. Huh7.5 cells growing on glass coverslips were transfected with Lipofectamine 2000 (11660-019, Invitrogen), according to the manufacturer's instructions. The cells were fixed in 3.7% formaldehyde in PBS (pH 7.4) for 30 min. Formaldehyde was quenched by incubating the cells for 30 min in 0.1 M glycine in 1× PBS. Then cells were


DOI: 10.1021/acs.biochem.7b01087
Biochemistry 2018, 57, 839−851

permeabilized using 0.1% Triton in PBS (pH 7.4) for 10 min at 25 °C and then incubated with the appropriate dilution of primary and secondary antibodies in PBS for 1 h and 45 min, respectively.

**Endocytosis Assay.** HuH7.5 cells growing on glass coverslips were transfected with HA-FZD4-wt. Twenty-four hours after being transfected, cells were incubated for 1 h at 4 °C in Leibovitz L15 Medium (L0300, Microgem) containing FBS 10%, in the presence or absence of the indicated concentration of FzM1.8. After being incubated, cells were warmed to 37 °C for 1 h, fixed in 3.7% formaldehyde, and processed for immunofluorescence.

**Alkaline Phosphatase Assay.** Alkaline phosphatase activity was measured by colorimetric detection of *p*-nitrophenol. After CaCo-2 cells had been cultured with the indicated compounds, cell culture medium was gently removed from the cultures and cells were washed twice with PBS. Cells were then incubated with a solution of 2.5 mg/mL *p*-nitrophenyl phosphate dissolved in 100 mM diethanolamine, 150 mM NaCl, and 2 mM $MgCl_2$ at pH 9.5 for 60 min. After the incubation, the solution was transferred to a new tube, and 0.17 M NaOH was added to stop the reaction. The absorbance was read at $OD_{405}$ in a microplate reader.

**Excision and Culturing of Human Biopsies from Familial Adenomatosis Poliposis (FAP) Patients.** Biopsies from FAP patients were kindly provided by G. B. Rossi. The study was approved by the Ethics Committee of the University of Naples Federico II. Immediately after excision, biopsies were rinsed in physiological saline. Samples were then digested with trypsin for 10 min at room temperature and centrifuged at 400 rpm for 10 min at room temperature. Isolated cells present in the supernatant were then counted and cultured at a confluency of 100000 cells/mL in DMEM supplemented with 10% FBS, Glutamax, and Pen/Strep. Where indicated, FzM1 and FzM1.8 were added at concentrations of 15 and 5 $\mu$M, respectively. After incubation for 24 and 48 h, cell viability was measured with the Trypan blue assay and propidium iodide.

**Statistical Analysis.** $EC_{50}$ values were calculated from dose−response data using nonlinear regression analysis of Prism version 6.0 (GraphPad, GraphPad Software, San Diego, CA). All data were analyzed using the two-tailed Student's *t* test. A two-way analysis of variance test was used to compare columns. *P* values of <0.05 were considered statistically significant.

***In Silico* FZD4 Model.** Three-dimensional (3D) *in silico* models of FZD4 in complex with G$\alpha$s and the hypothetical binding modes for FzM1 and FzM1.8 were generated using the CCP4 suite (CCP4 Software), as previously described.[15] The crystal structure of the smoothened receptor [Protein Data Bank (PDB) entries 4N4W and 4JKV][19] and the crystal structure of the $\beta$2 adrenergic receptor−G$\alpha_s$ protein complex (PDB entry 3SN6)[20]were both used as templates for the TMD of FZD4 and for the FZD4/G$\alpha$s models, respectively. $\beta$2 adrenergic receptor and FZD4 sequences were structurally aligned using the FFAS-3D and I-TASSER servers. Five 3D models of FZD4 were generated and scored using the available scoring functions of SPICKER and through visual inspections. The geometry of the final FZD4, FZD4/G$\alpha$s, FZD4/FzM1.8/G$\alpha$s, and FZD4/FzM1/G$\alpha$s complex models was optimized using several cycles of force field minimization. Cartoons were generated as previously described.[15]

## RESULTS AND DISCUSSION

**A Molecular Switch Converts FzM1 in Allosteric Agonist FzM1.8.** To induce a molecular switch in FzM1, we generated a small library of FzM1 analogues (Figure S1). We attempted mode switching by replacing the naphthyl, the phenol, the thiophene, or the ureidic linker of FzM1. The activity of the new compounds was assayed in HEK293 cells transiently expressing both FZD4 and a WNT reporter construct, the latter presenting the coding sequence of GFP under the control of an optimized WNT responsive element (WRE-wt). Compared to that of mock transfected cells, transient expression of FZD4 did not induce activation of the WNT reporter construct, indicating a low level of basal activity of FZD4 in the absence of ligands. On other hand, activation of the WNT/$\beta$-catenin canonical pathway by the GSK3-$\beta$ inhibitor LiCl (Figure S2A−C) or upon treatment with FZD4 agonist WNT-5A (below) induced GFP expression and increased the fluorescence of the cells. Replacement of FzM1 thiophene with either a carboxylic or a carboxyl ester group induced a molecular switch in the lead and transformed FzM1 into two new allosteric agonists of FZD4. In the absence of any orthosteric ligand, the two compounds 3-hydroxy-5-[3-(naphthalen-2-yl)ureido]benzoic acid [FzM1.8 (Figure 1A−C)] and 3-hydroxy-5-[3-(naphthalen-2-yl)ureido]benzoic acid [FzM1.10 (Figures S1−S3)] were able to increase WRE activity in FZD4-expressing HEK293 cells. All the other synthesized analogues of FzM1 (Figure S1) did not increase WRE activity and acted as WNT inhibitors (Figure S3). Like FzM1, FzM1.8 did not increase WRE activity in cells not expressing FZD4 (Figure S4C,D), indicating that the effect of the compound is dependent on FZD4. Moreover, FzM1.8 did not induce GFP expression in cells transiently expressing both FZD4 and either a mutated nonfunctional WRE reporter [WRE-mut (Figure S4E,F)] or a DNA construct in which a CMV promoter controls GFP expression [cmv-GFP (Figure S4G)]. These results confirm that FzM1.8 does not act as general transcriptional activator and that, instead, its activity relies on a functional WRE.

Interestingly, in the range of concentrations tested, the two compounds modulated WRE activity with values fitting hormetic dose−response curves (described in eq I).

$$\text{fluorescence} = \text{background} + \frac{\text{fluorescence max} - \text{background}}{1 + 10^{(\log EC_{50act} - \log[X]) \times \text{Hill slope}_{act}}} + \frac{\text{fluorescence max} - \text{background}}{1 + 10^{(\log EC_{50inh} - \log[X]) \times \text{Hill slope}_{inh}}} \quad \text{(I)}$$

For each of the two allosteric ligands, we measured both a stimulatory activity [for FzM1.8, $EC_{50}$ of activation (log $EC_{50act}$) ± the standard error of the mean (sem) = −6.4 ± 0.2; $n$ = 16] and an inhibitory activity [$EC_{50}$ of inhibition (log $EC_{50inh}$) ± sem = −5.5 ± 0.1; $n$ = 16] (Figure 1C). $EC_{50act}$ and $EC_{50inh}$ of the two compounds fall in the same concentration range (Figure 1C and Figure S3), with FzM1.8 presenting an efficacy of stimulation that is higher than that of FzM1.10.

Using site-directed mutagenesis and hydrogen-to-deuterium exchange (HDX) analysis, we have previously identified FZD-ICL3 as the site addressed by FzM1.[15] The compound contacts ICL3 residue Thr-425, and its binding reduces the solvent accessibility of this region of the receptor.[15] Despite presenting a switch in its activity, FzM1.8 contacts the same binding sites


DOI: 10.1021/acs.biochem.7b01087
*Biochemistry* 2018, 57, 839−851

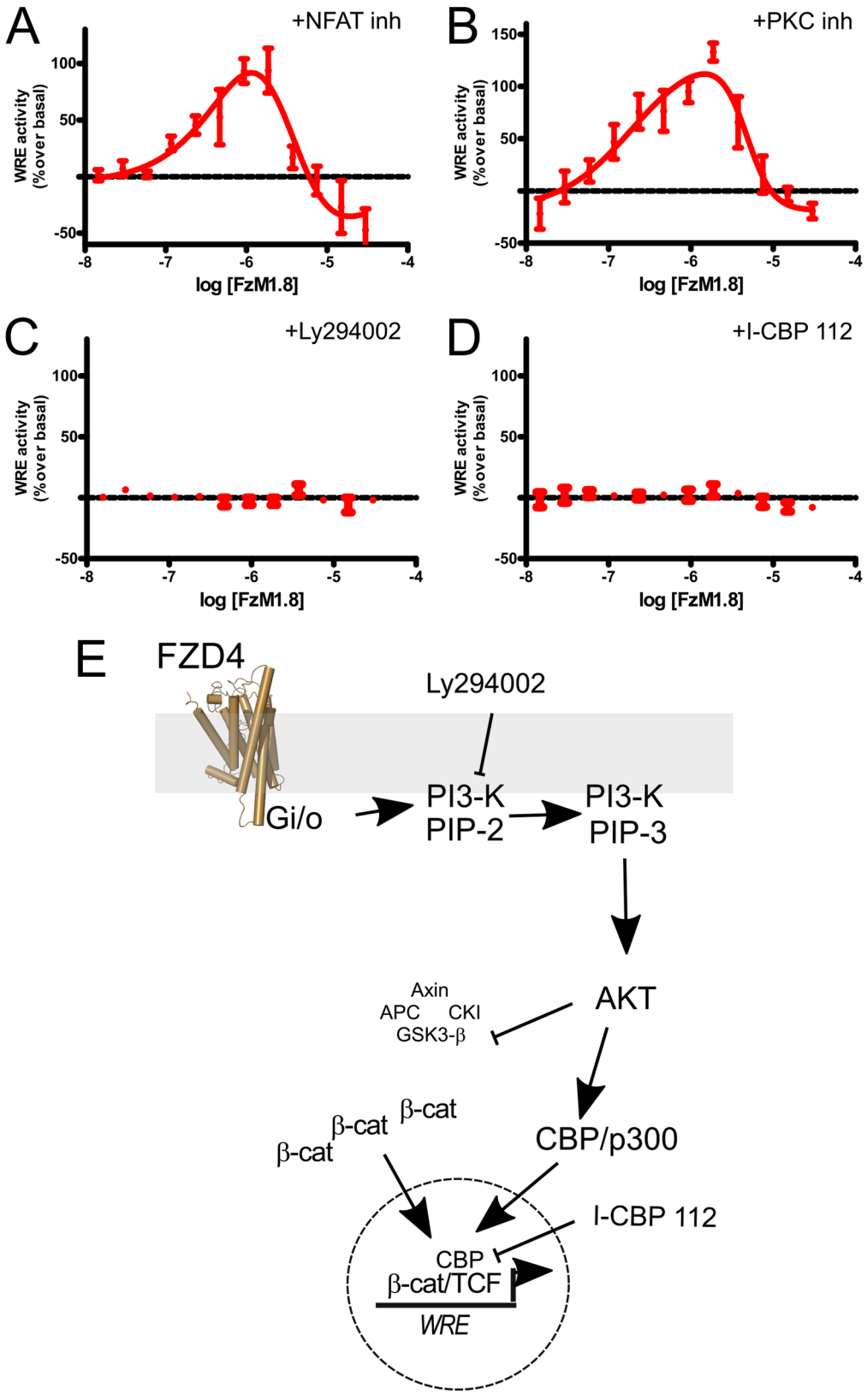


**Figure 2.** FZD4/FzM1.8 complex activates PI3K. (A–D) Dose–response curves for FzM1.8 modulation of WRE activity in cells expressing FZD4wt in the presence of NFAT, PKC, PI3K, and CBP/p300 inhibitors, respectively. (E) Schematic cartoon depicting the involvement of FZD4 in the WNT/PI3K pathway. Values are reported as means ± sem ($n$ = 5). *$P$ < 0.05.

of the original lead. As already shown for FzM1, HEK293 cells transfected with FZD4 mutant FZD4-T425A only partially responded to FzM1.8 treatment (Figure 1D). Moreover, HDX analysis reveals that FzM1.8 binding reduced the solvent accessibility of ICL3 (Figure S5 and Tables S1–S3). Interestingly, both ligands affected the conformation of TM6,



DOI: 10.1021/acs.biochem.7b01087
*Biochemistry* 2018, 57, 839–851

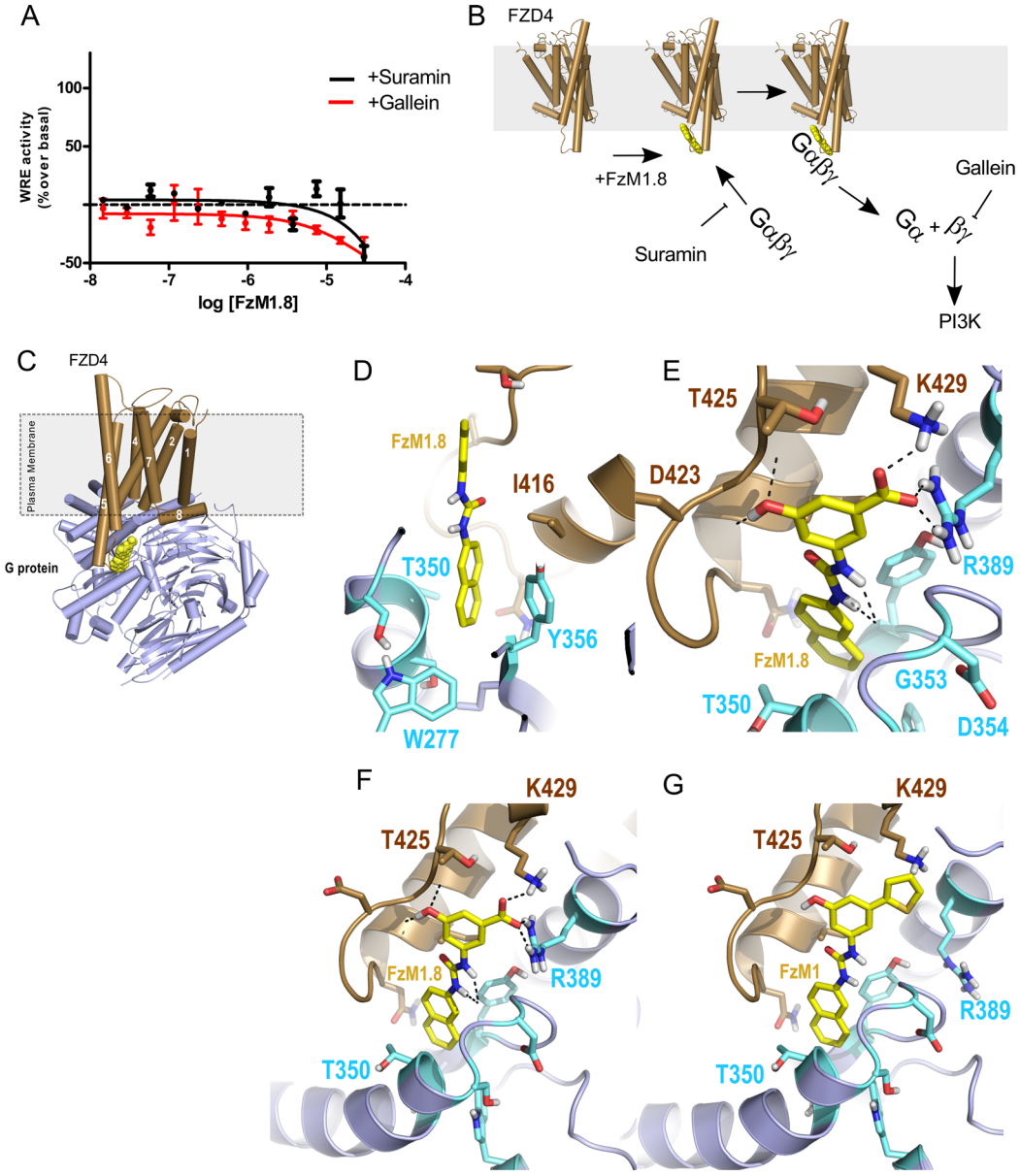


**Figure 3.** FzM1.8 activity involves G protein signaling. (A) Dose−response curves for FzM1.8 modulation of WRE activity in the presence of Suramin (black) or Gallein (red). (B) Schematic cartoon depicting the pathway elicited by FzM1.8 (yellow) upon binding to FZD4. (C) FZD4/FzM1.8/G$\alpha$ *in silico* model that inspired the mutants described herein: FZD4 transmembrane domain (brown cartoon, in which numbers indicate TM helices of FZD4), G$\alpha$ subunit (cyan cartoon), and FzM1.8 (yellow molecular surface) (FZD4 extracellular domain omitted for the sake of clarity). (D−G) Proposed mode of binding of FzM1.8 (yellow balls and sticks). The FzM1.8 binding site is located at the interface between FZD4 ICL3 (brown cartoon) and helices H3−H5 of the G$\alpha$ subunit (cyan cartoon). The negatively charged carboxyl group of FzM1.8 (H) but not the thiophene of FzM1 (I) contacts G$\alpha$-R389 on helix 5 of the G protein. Values are reported as means ± sem ($n$ = 5). *$P$ < 0.05.

with FzM1.8 increasing the solvent accessibility of this section of the receptor more than FzM1 did (Figure S5 and Tables S1−S3).

**Binding of FzM1.8 to FZD4 Initiates a Noncanonical WNT Signaling Route.** Treatments with FzM1.8 as short as 15 min were sufficient to achieve maximal activation of the WNT responsive elements. This timing was similar to that required by WNT5A (Figure 1E) and compatible with a signaling pathway originating soon after binding of the ligand to its cognate receptor.

Regardless, we performed a set of experiments to exclude other unrelated signaling explanations for modulation of FZD4 by FzM1.8. Below 30 $\mu$M and in the time window of the experiment (treatment for ≤48 h), FzM1.8 did not affect the HEK293 cell proliferation rate or induce cell death or apoptosis or arrest the growth of the cultures (Figure S6A−C). This proves that stimulation, as well as inhibition, of the WRE activity measured upon treatment with low and high concentrations of FzM1.8, did not depend on an increased level of duplication of the cells or the toxicity of the compound, two common causes of hormesis. FzM1.8 does not affect maturation or PM localization of FZD4. This was shown in HEK293 cells as well as in human hepatoma HuH7 cells, that for their flat shape better suits immunofluorescence studies of PM-localized proteins (Figure S7). Finally, in a manner different from that of FZD antagonist Niclosamide,[23] FzM1.8 did not induce FZD4 endocytosis (Figure S8).



DOI: 10.1021/acs.biochem.7b01087
*Biochemistry* 2018, 57, 839−851

Thus, upon binding to FZD4, allosteric agonist FzM1.8 initiates a signaling route resulting in increased WRE activity.

We started testing if FzM1.8, by either affecting FZD4/DVL interaction or inhibiting $\beta$-catenin proteasomal degradation, was acting via the WNT canonical pathway (Figure S9A). As shown in Figure S9B, in the presence of FzM1.8, FZD4 can still recruit DVL. Furthermore, in a manner different from that of WNT ligands or LiCl, FzM1.8 did not increase intracellular levels of $\beta$-catenin (Figure S9C). Finally, in the presence of CIK 7, a pan-inhibitor of casein kinase I,[21] a protein involved in activation of the FZD4/DVL complex,[22] FzM1.8 stimulatory activity was mostly preserved (Figure S9D). Thus, the FzM1.8/FZD4 complex stimulates WRE activity but does not affect proteins taking part in the FZD4/DVL/APC axis.

**The FZD4/FzM1.8 Complex Activates a WNT Signaling Route That Involves PI3K.** To explain FzM1.8 activity, we thus hypothesized the involvement of a noncanonical pathway. The WNT/$Ca^{2+}$, PCP, and WNT/ROR pathways are inhibitory toward the canonical WNT/$\beta$-catenin pathway, and thus, their involvement would not explain FzM1.8 stimulatory activity. Moreover, inhibition of two known modulators of the WNT/$Ca^{2+}$ pathway, PKC by bisindolylmaleimide[24] and NFAT by the NFAT inhibitor peptide,[25] had no effect on FzM1.8 activity (Figure 2A,B), further excluding the involvement of the WNT/$Ca^{2+}$ pathway.

The only pathway that has been described as a positive modulator of the WNT canonical pathway is the one involving phosphatidylinositol-4,5-bisphosphate 3-kinases (PI3Ks).[2] PI3K has been already shown to affect the WNT canonical pathway on multiple levels. In differentiated myofibers, binding of orthosteric ligand WNT7a to FZD7 directly activates the PI3K pathway and induces myofiber hypertrophy.[26] Moreover, via AKT, PI3K inhibits GSK3-$\beta$ and leads to $\beta$-catenin stabilization.[27] Alternatively, AKT has been shown to promote the activity of histone acetyltransferases CBP and P300, both trans-activators of the $\beta$-catenin/TCF transcription complex.[28] These remodel the chromatin bound to WNT responsive genes, ultimately boosting the activity of the $\beta$-catenin/TCF transcription complex. Indeed, in the presence of PI3K inhibitor Ly294002,[29] FzM1.8 lost its ability to induce WRE activity (Figure 2C). WB analysis of cells treated with FzM1.8 revealed an increase in the level of AKT phosphorylation at Thr-308 after incubation with the ligand for 30 min and 2 h, confirming the involvement of PI3K in the pathway activated by FzM1.8. Differently, we did not measure an increase in the level of AKT phosphorylation at Ser-473 (Figure S10). Finally, HEK293 cells expressing both FZD4 and the AKT dominant negative mutant AKT K179M were insensitive to FzM1.8, further proving the involvement of the protein kinase in the WRE activation elicited by the ligand (Figure S10).

Because FzM1.8 does not induce $\beta$-catenin stabilization (Figure S9C), we tested whether activation of WRE by FzM1.8 was dependent on CBP/p300. In the presence of the CBP/p300 specific inhibitor I-CBP 112,[30] FzM1.8 activity was drastically reduced (Figure 2D), confirming the involvement of PI3K and CBP/p300 downstream of the pathway activated by FzM1.8.

The involvement of CBP/p300 indicates also that the FZD4/PI3K axis elicited by FzM1.8 is "ancillary" to the canonical WNT pathway. Even if it bypasses the WNT/FZD/APC canonical route, the FZD4/PI3K axis acts ultimately on the nuclear pool of $\beta$-catenin (Figure 2E).

**Structural Details of FZD4/PI3K Axis Activation by FzM1.8.** PI3K activation by GPCRs involves heterotrimeric G proteins.[31] In the presence of Suramin, an inhibitor of G proteins binding to GPCRs,[32] treatment with FzM1.8 did not increase WRE basal levels (Figure 3A), suggesting that FzM1.8 stimulates the assembly of a FZD4/heterotrimeric G protein complex. Interestingly, the inhibitor of G$\beta\gamma$ activity, Gallein,[33] also abolished FzM1.8 activity (Figure 3A). PI3K activation by the FzM1.8/FZD4 complex thus requires binding of heterotrimeric G proteins, activation of the latter, and consequent release of the $\beta\gamma$ subunit (Figure 3B). In the basal state, FZD4 is inactive (Figure S2). When an allosteric ligand imposes a specific conformation on the cognate receptor and forces it to elicit a specific pathway, it is said to be endowed with signal bias activity. Very likely, binding of FzM1.8 to ICL3 of FZD4 stabilizes a FZD4 conformation with increased affinity for heterotrimeric G proteins. Probably, FzM1.8 binding increases the GTP exchange factor (GEF) activity of FZD4, causing the release of the $\beta\gamma$ subunit, which in turn activates PI3K.

To confirm our model, we generated a set of FZD4 mutants to mimic a FzM1.8-bound FZD4 conformation. To choose the right amino acid substitutions, we built an *in silico* model for the FZD4/FzM1.8/G protein complex. The closest receptor to use as a possible FZD4 template would have definitely been the human class F GPCR smoothened receptor (Smo), whose crystal structures in complex with several of its orthosteric ligands have been recently disclosed.[19] However, none of these structures are in complex with a G protein, and more importantly, the electron density for ICL3 of Smo is missing in almost all deposited structures of Smo. We thus decided to generate a 3D model of FZD4 using as an additional template the only available crystal structure of a GPCR/G protein complex, the $\beta$2 adrenergic receptor/G$\alpha_s$ protein complex (PDB entry 3SN6)[20] (Figure 3E). FzM1.8 binds to ICL3 of FZD4, contacting Thr-425 of the receptor (Figure 1D), and thus, docking of FzM1.8 was focused on a pocket formed by FZD4 ICL3 and the G$\alpha$ subunit.[34] The resulting hypothetical binding mode is depicted in Figure 3D−G. The naphthyl moiety of FzM1.8 lies in a small apolar pocket formed by G$\alpha$-Y358$^{G.h4s6.20}$ (CGN, common G$\alpha$ numbering), G$\alpha$-W277$^{G.H3.13}$, and G$\alpha$-T350$^{G.h4s6.3}$ and by FZD4 I416. The ureidic linker contacts G$\alpha$-G353$^{G.h4s6.9}$. The hydroxyl of the phenol ring contacts FZD4 T425 and FZD4 D423. Finally, the carboxyl moiety of FzM1.8 addresses FZD4 K249 and G$\alpha$ R389$^{G.H5.21}$. In our models, the negatively charged carboxyl group of FzM1.8 but not the thiophene of FzM1 contacts R389$^{G.H5.21}$. The G.h5.21 residue is highly conserved in all the G$\alpha$ paralogues and is essential for both GTP/GDP exchange and dissociation of the $\beta/\gamma$ subunit.[35,36]

**A FZD4-wt/FZD4-T425D Heterocomplex Mimics FZD4-wt Bound to FzM1.8.** According to our *in silico* model, the negative charge of FzM1.8 increases FZD4 GEF activity by contacting a conserved positive residue on helix H5 of the G$\alpha$ subunit. We thus attempted to mimic a FZD4/FzM1.8 complex by generating a FZD4 mutant in which Thr-425 was replaced with a negatively charged Asp residue.

When expressed in cells, FZD4-T425D folds properly as shown by its correct intracellular localization on the PM of the cells (Figure S11). Moreover, the mutant can still recruit DVL, indicating that the amino acid substitution did not affect FZD4/DVL interaction (Figure S12). Like the FZD-T425A mutant (Figure 1D), FZD4-T425D does not respond to FzM1.8 treatment (Figure 4A), very likely because of the



DOI: 10.1021/acs.biochem.7b01087
*Biochemistry* 2018, 57, 839−851

repulsion between the negative charge of FzM1.8 and the side chain of D425.

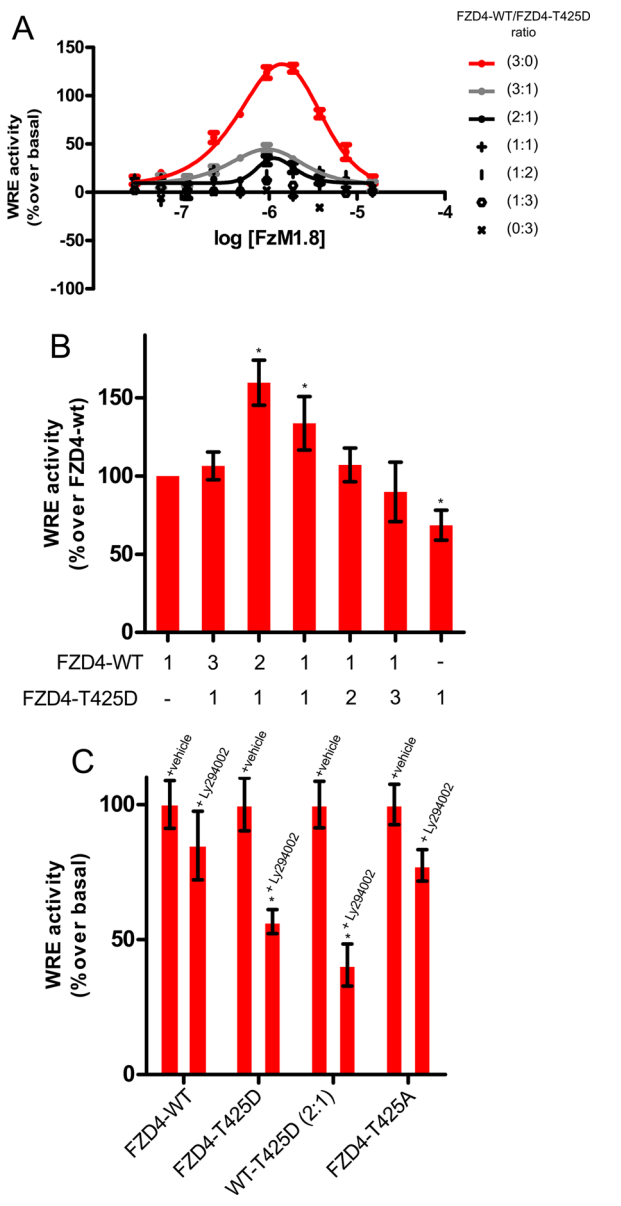


**Figure 4.** Mutant FZD4-T425D mimics FZD4 bound to FZM1.8. (A) Dose−response curves for FzM1.8 modulation of WRE activity in cells transfected with cDNA encoding FZD4wt (red dots), FZD4-T425D (stars), or a mixture of them. FZD4wt:FZD4-T425D cDNA ratios of 3:1 (gray dots), 2:1 (●), 1:1 (+), 1:2 (|), and 1:3 (○). (B) Effect of co-expression of FZD4wt and FZD4-T425D at different ratios on basal WRE activity. (C) Effect of Ly294002 on the basal WRE activity elicited in HEK293 cells by the expression of FZD4wt, FZD4-T425D, and FZD4-T425A homo-oligomers or FZD4wt/FZD4-T425D hetero-oligomers. In panel A, values are reported as means ± the standard deviation ($n$ = 5); in panels B and C, values are reported as means ± sem ($n$ = 5). *$P$ < 0.05.

Cells transfected with only FZD4-T425D did not present an increased WRE basal activity (Figure 4B); on the contrary, they presented a diminished one. Thus, FZD4-T425D does not mimic a FZD4-wt/FzM1.8 complex. However, because FZD4-wt is an obligate oligomer,[37,38] we moved to co-express FZD4-T425D and FZD4-wt to ultimately test how the WRE basal activity and the response to FzM1.8 were influenced by FZD4-wt/FZD4-T425D hetero-oligomers.

FZD4-T425D exerted a dominant negative effect on FZD4-wt signaling elicited by FzM1.8. Co-transfection of HEK293 cells with a mixture of cDNAs encoding FZD4-wt and FZD4-T425D in a 3:1 ratio, despite strongly favoring expression of the wt receptor, impaired the response of FZD4 to FzM1.8 treatment (Figure 4A). This suggests that the oligomeric state of FZD4 influences the response to FzM1.8.

Differently, as shown in Figure 4B, WRE basal activity was favored by the co-expression of FZD4-wt with FZD4-T425D. In the absence of the agonist, a 2:1 ratio of FZD4-wt to FZD4-T425D was enough to induce WRE basal activity. Moreover, such activity was sensitive to Ly294002 (Figure 4C), indicating the pathway activated by the hetero-oligomer is partially relying on the FZD4/PI3K axis. Thus, mutant FZD4-T425D seems to indeed mimic a FZD4/FzM1.8 complex because it biases FZD4 signaling toward the same PI3K pathway elicited by binding of FzM1.8 to FZD4. However, it does so only when it forms, together with FZD4-wt, a FZD4-wt/FZD4-T425D hetero-complex.

**FzM1.8 Acts as a NAM for FZD4 Signaling Elicited by WNT5A.** Many allosteric agonists are endowed with Ago-PAM or Ago-NAM activity; i.e., they can modulate downstream signaling events and simultaneously affect binding of their cognate receptors to orthosteric ligands. To prove FzM1.8 is an Ago-PAM or an Ago-NAM for FZD4, we measured the effect of FzM1.8 treatment[39] on the WRE activity induced by a FZD4 orthosteric ligand, the protein WNT5A. Activation by the agonist was dependent on FZD4 and on the presence of a wild-type TCF/LEF promoter. As shown in Figure S13, when FZD4-expressing HEK293 cells were incubated with WNT5A-conditioned medium,[40] WRE activity increased.

FZD4-expressing cells were treated with WNT5A-conditioned medium in the presence of either FzM1 or FzM1.8. FzM1 works efficiently as a NAM for FZD4 and reduces WNT5A-dependent WRE activity [log $EC_{50inh}$ ± sem = −6.2 ± 0.2 (Figure 5A)].[15,41] Differently, in the presence of WNT5A, FzM1.8 modulates WRE activity (Figure 5B) with dose−response values fitting a hormetic triphasic curve (described in eq II).

$$\text{fluorescence} = \text{background} + \frac{\text{fluorescence max} - \text{background}}{1 + 10^{(\log EC_{50act} - \log[X]) \times \text{Hill slope}_{act}}} + \frac{\text{fluorescence max} - \text{background}}{1 + 10^{(\log EC_{50inh} - \log[X]) \times \text{Hill slope}_{inh}}} + \frac{\text{fluorescence max} - \text{background}}{1 + 10^{(\log EC_{50inh2} - \log[X]) \times \text{Hill slope}_{inh2}}} \quad \text{(II)}$$

Two distinct inhibitory phases [log $EC_{50inh1}$ ± sem = −5.5 ± 0.2, and log $EC_{50inh2}$ ± sem = −7.8 ± 0.2 ($n$ = 16)] are interwoven with a stimulatory one [log $EC_{50act}$ ± sem = −6.7 ± 0.1 ($n$ = 16)]. The bell-shaped section of the dose−response curve (−6.5 < log[FzM1.8] < −5.5) is independent of WNT5A and is the result of FzM1.8 allosteric agonist activity. When FzM1.8 treatment was performed in the presence of both WNT5A and Ly294002, this section of the dose−response curve disappeared (Figure 5D). A comparison of the FzM1.8 dose−response curves measured in the presence (Figure 5C) and absence (Figure 1C) of WNT5A reveals that $EC_{50act}$ and $EC_{50inh}$, as well as the WRE stimulatory efficacy of FzM1.8, are


DOI: 10.1021/acs.biochem.7b01087
Biochemistry 2018, 57, 839−851

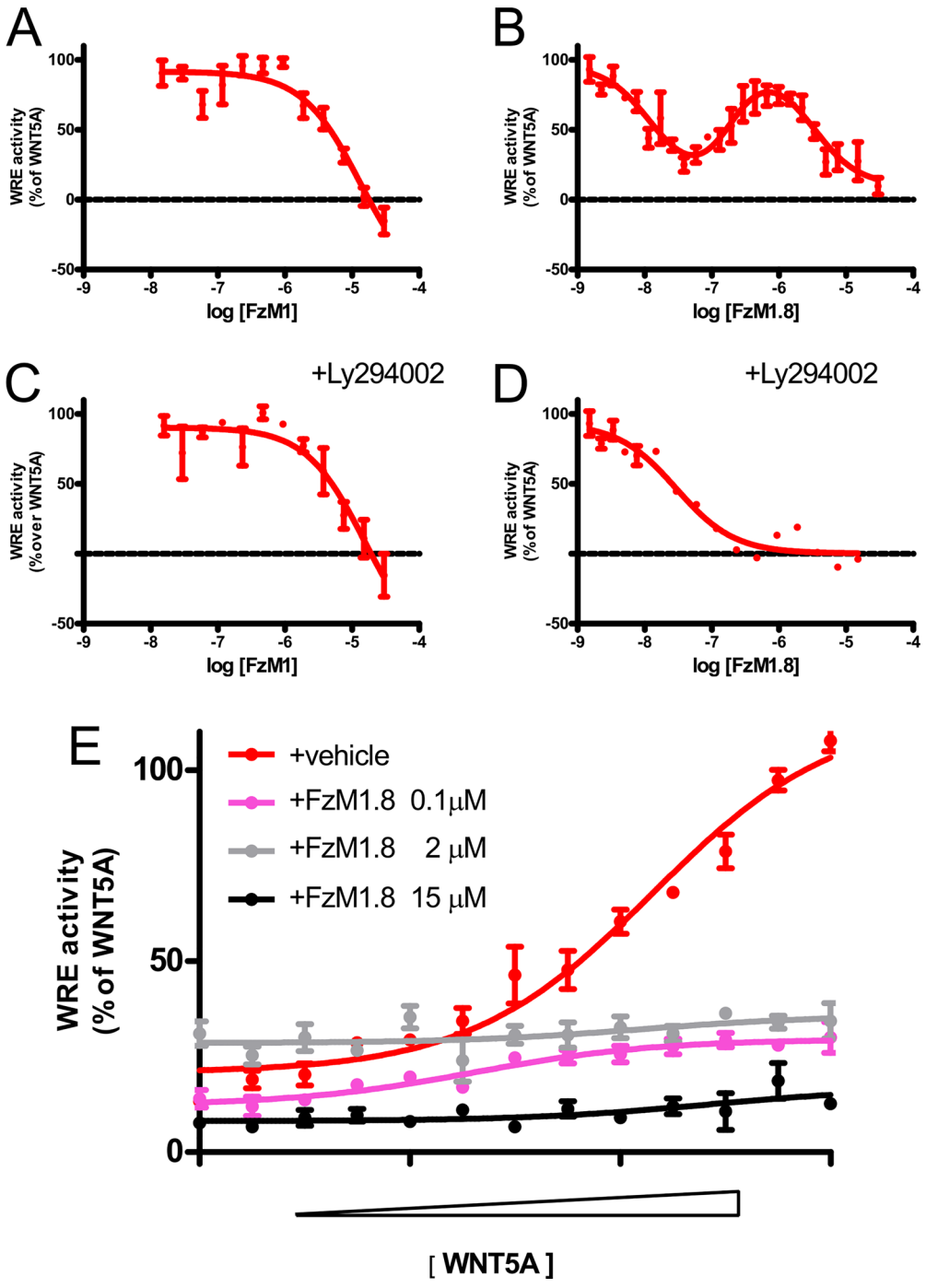


**Figure 5.** FzM1.8 acts as NAM for FZD4 signaling elicited by WNT5A. (A and B) Dose−response curves for FzM1 and FzM1.8 modulation, respectively, of WRE activity elicited by WNT5A. Values indicate changes in WRE activity (expressed as a percentage of change over pure WNT5A activity). (C and D) Dose−response curves for FzM1 and FzM1.8 modulation, respectively, of WRE activity elicited by WNT5A in the presence of Ly294002. (E) Dose−response curves for WNT5A modulation of WRE activity in the presence of DMSO or the indicated amount of FzM1.8. Values are reported as means ± sem ($n$ = 5). *$P$ < 0.05.

only minimally altered by the presence of the orthosteric agonist. This indicates that WNT5A binding does not affect, by increasing or decreasing, FzM1.8-dependent signaling.

We thus moved to record dose−response curves of WNT5A in the presence of a fixed concentration of FzM1.8 (Figure 5E). Incubation with the allosteric ligand decreased the potency of WNT5A, indicating that FzM1.8 acts as a NAM for FZD4 signaling elicited by WNT5A.

Why, in the presence of Ly294002, is the WNT5A potency not fully restored (Figure 5D)? While FzM1.8 stimulatory activity is blocked by the PI3K inhibitor, WNT5A is inhibited by the molecule (Figure 5D). This is very likely the result of the NAM activity of FzM1.8 toward WNT5A. Ly294002 does not block the binding of FzM1.8 to FZD4, only the intracellular pathway elicited by the event of binding. Despite the fact that FZD4/PI3K signaling is not active, FzM1.8 can still bind to



DOI: 10.1021/acs.biochem.7b01087
*Biochemistry* 2018, 57, 839−851

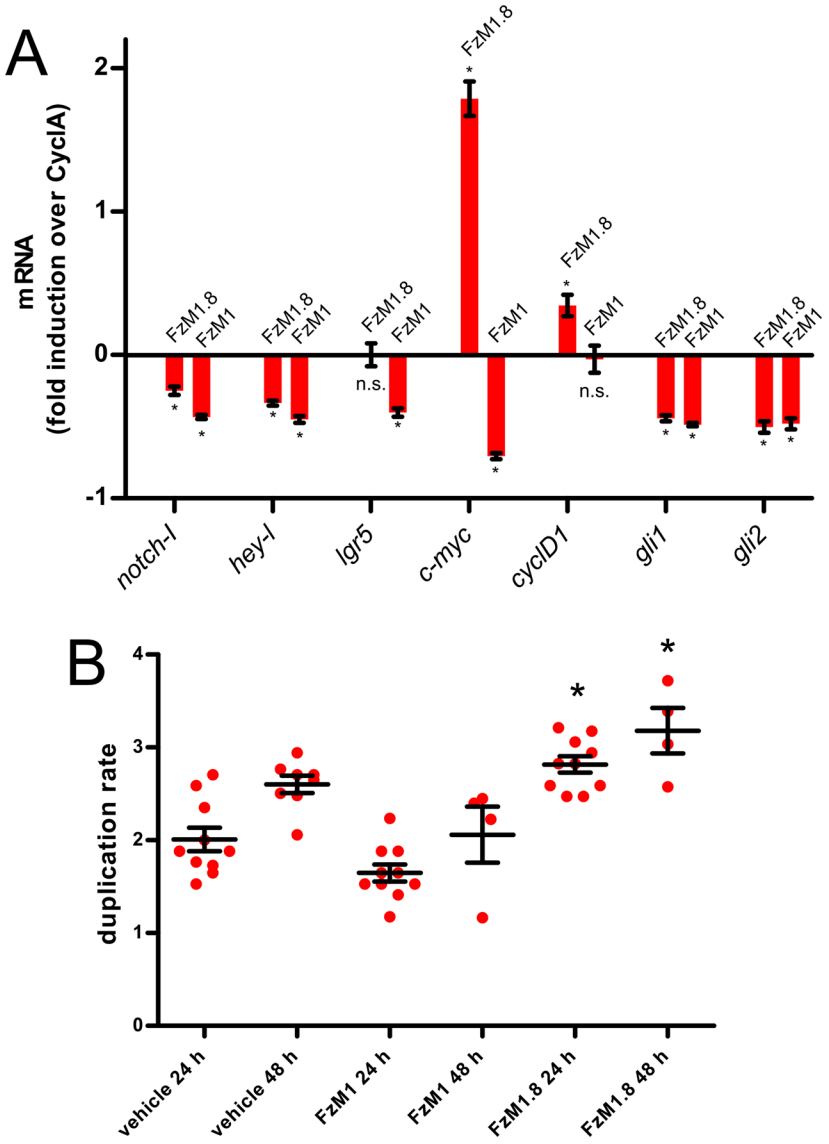


**Figure 6.** FzM1.8 reduces the stemness and increases the rate of proliferation of undifferentiated colon cancer cells. (A) Effect of FzM1.8 or FzM.1 on the expression levels of the WNT (*lgr5*, *c-myc*, and *cyclin-D1*), Notch (*notchI* and *hey-l*) and of the Sonic hedgehog (*gli1* and *gli2*) target genes in CaCo-2 cells. mRNA levels were normalized to those of *cyclophilin A*. (B) Rate of duplication of human colonic biopsies in culture medium supplemented with FzM1, FzM1.8, or vehicle. Values are expressed as means ± sem (in panels A and B, $n = 3$). *$P < 0.05$.

FZD4 and act as a NAM toward WNT5A, hampering the canonical signaling elicited by the orthosteric agonist.

**The FZD4/PI3K Axis Preserves the Stemness and Sustains the Proliferation of Undifferentiated Cells.** To follow at the cellular level the results of the activation of the FZD4/PI3K pathway by FzM1.8, we used *in vitro* cultured CaCo-2 cells. These express endogenous FZD4,[42] and as we have already shown, they respond to FzM1 treatment.[15] Upon treatment with FzM1.8, WNT responsive genes *c-myc* and *cycl-D1* were upregulated (Figure 6A). On the other hand, FzM1.8 treatment left unaltered the expression of colon stem cell marker *lgr5*, indicating that the FZD4/PI3K pathway stimulates proliferation and preserving the stemness of the cells. FzM1.8 treatment reduces the level of expression of Notch and Sonic Hedgehog specific genes pointing toward FzM1.8 specificity toward the WNT pathway and a competition between the FZD4/PI3K axis and the Notch and Sonic Hedgehog pathway (Figure 6A). Despite promoting proliferation, FzM1.8 treatment did not induce differentiation of CaCo-2 cells as indicated by the timing of the appearance of the colonic differentiation marker alkaline phosphatase (Figure S13) that was not influenced by FzM1.8 treatment.

Finally, the results obtained in CaCo-2 cells were confirmed in an *ex vivo* system. Mutations in the *APC* gene occur very commonly in patients affected by FAP.[43] This genetic disease is characterized by a hyperactive WNT pathway resulting in the proliferation of undifferentiated progenitors of the colon crypt and formation of colonic polyps.[1] The latter transform with high frequency into adenocarcinomas. Human colon biopsies were cultured *in vitro* soon after their resection from FAP patients. In unsupplemented media, these *ex vivo* samples duplicate poorly and their growth is rapidly arrested. As expected, treatment with FzM1 resulted in a decreased rate of survival of the cultures. Differently, supplementation of the culture medium with FzM1.8 resulted in increased rates of survival and proliferation of the cells (Figure 6B).



DOI: 10.1021/acs.biochem.7b01087
*Biochemistry* 2018, 57, 839−851

## CONCLUSIONS

Approaching the study of the WNT signaling is a difficult task. The huge plethora of different biological processes in which the pathway is involved, the many interconnected signaling routes originating upon binding of a WNT to FZD, and the existence of different WNT/FZD combinations, of FZD oligomers, and of co-receptors all contribute and make this intracellular pathway fascinating but complex.

Pure and biologically active WNT proteins are difficult to obtain because of their lipoprotein nature. The composition of the widely used WNT-conditioned media is not known and thus difficult to control. In this scenario, small organic molecules acting as orthosteric or allosteric agonists for FZDs represent missing milestones in the WNT signaling field. These could be used in replacement of WNT proteins during *in vitro* functional studies, reducing costs and the complexity of production, or *in vivo* as drugs to either inhibit or activate the WNT pathway.[41]

We here present FzM1.8, a small organic allosteric agonist of FZD4. In the absence of any WNT ligand, FzM1.8 binds to FZD4 and activates the WNT/$\beta$-catenin pathway by promoting TCF/LEF transcriptional activity.

FzM1.8 acts by biasing FZD4 signaling toward a non-canonical route that involves PI3K. FzM1.8 binding stabilizes FZD4 in a conformational state with an increased affinity for heterotrimeric G proteins and stimulates the release of the G$\beta\gamma$ subunit that in turn activates PI3K. The activity seems to depend on the negative charge that the carboxylic moiety of FzM1.8 imposes on ICL3 of FZD4.

Dose−response curves for FZD4 modulation by FzM1.8 are bell-shaped. A very interesting hypothesis explaining this behavior would be the existence of compensatory actions of the ligand (e.g., desensitization and receptor downregulation) as well as indirect modulation of WRE activity (synthesis or degradation of regulatory proteins) or even a negative feedback response that becomes activated at high concentrations of FzM1.8.

However, the results obtained with the mutant FZD4-T425D point toward a similarly possible yet different explanation of the bell-shaped dose−response curve. This could arise as a result of partial and full occupancy of a FZD4 oligomer. The mutant FZD4-T425D activates the WNT/PI3K axis only when co-expressed with FZD4wt. On the other hand, when expressed alone, it neither responds to FzM1.8 nor presents increased basal WRE activity. This could be explained by (i) the heterocomplex mimicking a FZD4-wt oligomer partially occupied by FzM1.8 and (ii) a FZD4-T425D homocomplex mimicking a fully occupied oligomer. In this scenario, the inhibition we registered upon treatment with a high concentration of FzM1.8 could arise upon full occupancy of FZD4 oligomers. Probably when full occupancy occurs, each FZD4 protomer recruits a heterotrimeric G protein devoting the entire oligomer exclusively to the FZD4/PI3K axis. This has been already shown for FZD4. Overexpression of G proteins inhibits the WNT pathway as consequence of loss of the correct stoichiometry between FZD oligomers and intracellular proteins.[44]

Despite the complexity of explaining the mechanistic details underpinning the intracellular response to the allosteric ligand, FzM1.8 will offer us a great opportunity to illuminate, in the intricate complexity of the WNT/FZD signaling network, one specific WNT route, reducing the level of interference of the many other pathways of which FZD4 could be a part. Using FzM1.8 as a lead, new analogues will allow the development of new allosteric molecules selectively recruiting other intracellular effectors and biasing the WNT pathway toward different intracellular signaling routes.

## ASSOCIATED CONTENT

### Supporting Information

The Supporting Information is available free of charge on the ACS Publications website at DOI: 10.1021/acs.biochem.7b01087.

Figures S1−S14 and Tables S1−S3 (PDF)

Supporting experimental procedures and characterization of all compounds (PDF)

## AUTHOR INFORMATION


### Corresponding Authors

*Department of Pharmacy, Laboratory of Molecular Biology, University of Napoli Federico II, Napoli Italy Via Domenico Montesano 49, 80131 Napoli, Italy. Phone: +39 081 678117. E-mail: mariano.stornaiuolo@unina.it.

*Department of Pharmacy, University of Napoli Federico II, Napoli Italy Via Domenico Montesano 49, 80131 Napoli, Italy. E-mail: ettore.novellino@unina.it.

### ORCID

Giuseppe La Regina: 0000-0003-3252-1161

Antonella Accardo: 0000-0002-7899-2359

Romano Silvestri: 0000-0003-2489-0178

Ettore Novellino: 0000-0002-2181-2142

Mariano Stornaiuolo: 0000-0003-2200-5083

### Author Contributions

G.R. and S.B. contributed equally to this work.



### Funding

This work was financed by AIRC, Associazione Italiana Ricerca sul Cancro (MFAG 17651 to M.S.).


### Notes

The authors declare no competing financial interest.


## ACKNOWLEDGMENTS

The authors thank Salvatore Flora and Alessandra Salierno for technical help. The authors thank Prof. G. Condorelli and Prof. Santoro for sharing the DNA construct for AKT expression and G. Fiume (University Magna Graecia, Catanzaro, Italy) and Prof. A. Ianaro (University of Naples Federico II) for sharing the AKT antibodies.


## REFERENCES


(1) Clevers, H., and Nusse, R. (2012) Wnt/$\beta$-catenin signaling and disease. *Cell 149*, 1192.

(2) Dijksterhuis, J. P., Petersen, J., and Schulte, G. (2014) WNT/Frizzled signalling: Receptor-ligand selectivity with focus on FZD-G protein signalling and its physiological relevance: IUPHAR Review 3. *Br. J. Pharmacol. 171*, 1195−1209.

(3) Miki, T., Yasuda, S., and Kahn, M. (2011) Wnt/$\beta$-catenin signaling in embryonic stem cell self-renewal and somatic cell reprogramming. *Stem Cell Rev. 7*, 836−46.

(4) Krausova, M., and Korinek, V. (2014) Wnt signaling in adult intestinal stem cells and cancer. *Cell. Signalling 26*, 570−579.

(5) Schulte, G. (2015) Frizzleds and WNT/$\beta$-catenin signaling - The black box of ligand-receptor selectivity, complex stoichiometry and activation kinetics. *Eur. J. Pharmacol. 763*, 191−195.

(6) Cadigan, K. M. (2012) TCFs and Wnt/β-catenin Signaling. More than One Way to Throw the Switch. *Curr. Top. Dev. Biol. 98*, 1−34.
(7) Egger-Adam, D., and Katanaev, V. L. (2008) Trimeric G protein-dependent signaling by Frizzled receptors in animal development. *Front. Biosci., Landmark Ed. 13*, 4740−4755.
(8) Nichols, A. S., Floyd, D. H., Bruinsma, S. P., Narzinski, K., and Baranski, T. J. (2013) Frizzled receptors signal through G proteins. *Cell. Signalling 25*, 1468−1475.
(9) Gao, C., and Chen, Y. G. (2010) Dishevelled: The hub of Wnt signaling. *Cell. Signalling 22*, 717−727.
(10) Lai, S.-L., Chien, A. J., and Moon, R. T. (2009) Wnt/Fz signaling and the cytoskeleton: potential roles in tumorigenesis. *Cell Res. 19*, 532−545.
(11) Janda, C. Y., Waghray, D., Levin, a. M., Thomas, C., and Garcia, K. C. (2012) Structural Basis of Wnt Recognition by Frizzled. *Science (Washington, DC, U. S.) 337*, 59−64.
(12) Ye, X., Wang, Y., Cahill, H., Yu, M., Badea, T. C., Smallwood, P. M., Peachey, N. S., and Nathans, J. (2009) Norrin, Frizzled-4, and Lrp5 Signaling in Endothelial Cells Controls a Genetic Program for Retinal Vascularization. *Cell 139*, 285−298.
(13) Kimelman, D., and Xu, W. (2006) β-Catenin destruction complex: insights and questions from a structural perspective. *Oncogene 25*, 7482−7491.
(14) Wootten, D., Christopoulos, A., and Sexton, P. M. (2013) Emerging paradigms in GPCR allostery: implications for drug discovery. *Nat. Rev. Drug Discovery 12*, 630−644.
(15) Generoso, S. F., Giustiniano, M., La Regina, G., Bottone, S., Passacantilli, S., Di Maro, S., Cassese, H., Bruno, A., Mallardo, M., Dentice, M., Silvestri, R., Marinelli, L., Sarnataro, D., Bonatti, S., Novellino, E., and Stornaiuolo, M. (2015) Pharmacological folding chaperones act as allosteric ligands of Frizzled4. *Nat. Chem. Biol. 11*, 280−286.
(16) Schwartz, T. W., and Holst, B. (2007) Allosteric enhancers, allosteric agonists and ago-allosteric modulators: where do they bind and how do they act? *Trends Pharmacol. Sci. 28*, 366−373.
(17) Dror, R. O., Green, H. F., Valant, C., Borhani, D. W., Valcourt, J. R., Pan, A. C., Arlow, D. H., Canals, M., Lane, J. R., Rahmani, R., Baell, J. B., Sexton, P. M., Christopoulos, A., and Shaw, D. E. (2013) Structural basis for modulation of a G-protein-coupled receptor by allosteric drugs. *Nature 503*, 295−299.
(18) Lindsley, C. W., Emmitte, K. A., Hopkins, C. R., Bridges, T. M., Gregory, K. J., Niswender, C. M., and Conn, P. J. (2016) Practical Strategies and Concepts in GPCR Allosteric Modulator Discovery: Recent Advances with Metabotropic Glutamate Receptors. *Chem. Rev. 116*, 6707−6741.
(19) Wang, C., Wu, H., Katritch, V., Han, G. W., Huang, X.-P., Liu, W., Siu, F. Y., Roth, B. L., Cherezov, V., and Stevens, R. C. (2013) Structure of the human smoothened receptor bound to an antitumour agent. *Nature 497*, 338−343.
(20) Rasmussen, S. G. F., DeVree, B. T., Zou, Y., Kruse, A. C., Chung, K. Y., Kobilka, T. S., Thian, F. S., Chae, P. S., Pardon, E., Calinski, D., Mathiesen, J. M., Shah, S. T. A., Lyons, J. A., Caffrey, M., Gellman, S. H., Steyaert, J., Skiniotis, G., Weis, W. I., Sunahara, R. K., and Kobilka, B. K. (2011) Crystal structure of the β2 adrenergic receptor−Gs protein complex. *Nature 477*, 549−555.
(21) Osakada, F., Jin, Z.-B., Hirami, Y., Ikeda, H., Danjyo, T., Watanabe, K., Sasai, Y., and Takahashi, M. (2009) In vitro differentiation of retinal cells from human pluripotent stem cells by small-molecule induction. *J. Cell Sci. 122*, 3169−79.
(22) Cruciat, C.-M. (2014) Casein kinase 1 and Wnt/β-catenin signaling. *Curr. Opin. Cell Biol. 31*, 46−55.
(23) Chen, W. (2003) Dishevelled 2 Recruits -Arrestin 2 to Mediate Wnt5A-Stimulated Endocytosis of Frizzled 4. *Science (Washington, DC, U. S.) 301*, 1391−1394.
(24) Toullec, D., Pianetti, P., Coste, H., Bellevergue, P., Grand-Perret, T., Ajakane, M., Baudet, V., Boissin, P., Boursier, E., and Loriolle, F. (1991) The bisindolylmaleimide GF 109203X is a potent and selective inhibitor of protein kinase C. *J. Biol. Chem. 266*, 15771−15781.
(25) Roehrl, M. H. A., Kang, S., Aramburu, J., Wagner, G., Rao, A., and Hogan, P. G. (2004) Selective inhibition of calcineurin-NFAT signaling by blocking protein-protein interaction with small organic molecules. *Proc. Natl. Acad. Sci. U. S. A. 101*, 7554−7559.
(26) von Maltzahn, J., Bentzinger, C. F., and Rudnicki, M. A. (2012) Wnt7a−Fzd7 signalling directly activates the Akt/mTOR anabolic growth pathway in skeletal muscle. *Nat. Cell Biol. 14*, 186−191.
(27) Kim, S. E., Lee, W. J., and Choi, K. Y. (2007) The PI3 kinase-Akt pathway mediates Wnt3a-induced proliferation. *Cell. Signalling 19*, 511−518.
(28) Li, J., Sutter, C., Parker, D. S., Blauwkamp, T., Fang, M., and Cadigan, K. M. (2007) CBP/p300 are bimodal regulators of Wnt signaling. *EMBO J. 26*, 2284−2294.
(29) Thorpe, L. M., Yuzugullu, H., and Zhao, J. J. (2014) PI3K in cancer: divergent roles of isoforms, modes of activation and therapeutic targeting. *Nat. Rev. Cancer 15*, 7−24.
(30) Gallenkamp, D., Gelato, K. A., Haendler, B., and Weinmann, H. (2014) Bromodomains and their pharmacological inhibitors. *ChemMedChem 9*, 438−464.
(31) Vanhaesebroeck, B., Guillermet-Guibert, J., Graupera, M., and Bilanges, B. (2010) The emerging mechanisms of isoform-specific PI3K signalling. *Nat. Rev. Mol. Cell Biol. 11*, 329−341.
(32) Koval, A., Ahmed, K., and Katanaev, V. L. (2016) Inhibition of Wnt signalling and breast tumour growth by the multi-purpose drug suramin through suppression of heterotrimeric G proteins and Wnt endocytosis. *Biochem. J. 473*, 371−381.
(33) Bonacci, T. M., Mathews, J. L., Yuan, C., Lehmann, D. M., Malik, S., Wu, D., Font, J. L., Bidlack, J. M., and Smrcka, A. V. (2006) Differential targeting of Gbetagamma-subunit signaling with small molecules. *Science 312*, 443−446.
(34) Stornaiuolo, M., La Regina, G., Passacantilli, S., Grassia, G., Coluccia, A., La Pietra, V., Giustiniano, M., Cassese, H., Di Maro, S., Brancaccio, D., Taliani, S., Ialenti, A., Silvestri, R., Martini, C., Novellino, E., and Marinelli, L. (2015) Structure-based lead optimization and biological evaluation of BAX direct activators as novel potential anticancer agents. *J. Med. Chem. 58*, 2135−2148.
(35) Flock, T., Ravarani, C. N. J., Sun, D., Venkatakrishnan, A. J., Kayikci, M., Tate, C. G., Veprintsev, D. B., and Babu, M. M. (2015) Universal allosteric mechanism for Gα activation by GPCRs. *Nature 524*, 173−179.
(36) Oldham, W. M., and Hamm, H. E. (2008) Heterotrimeric G protein activation by G-protein-coupled receptors. *Nat. Rev. Mol. Cell Biol. 9*, 60−71.
(37) Robitaille, J., MacDonald, M. L. E., Kaykas, A., Sheldahl, L. C., Zeisler, J., Dubé, M.-P., Zhang, L.-H., Singaraja, R. R., Guernsey, D. L., Zheng, B., Siebert, L. F., Hoskin-Mott, A., Trese, M. T., Pimstone, S. N., Shastry, B. S., Moon, R. T., Hayden, M. R., Goldberg, Y. P., and Samuels, M. E. (2002) Mutant frizzled-4 disrupts retinal angiogenesis in familial exudative vitreoretinopathy. *Nat. Genet. 32*, 326−330.
(38) Lemma, V., D'Agostino, M., Caporaso, M. G., Mallardo, M., Oliviero, G., Stornaiuolo, M., and Bonatti, S. (2013) A disorder-to-order structural transition in the COOH-tail of Fz4 determines misfolding of the L501fsX533-Fz4 mutant. *Sci. Rep. 3*, 2659.
(39) Mikels, A. J., and Nusse, R. (2006) Purified Wnt5a Protein Activates or Inhibits β-Catenin−TCF Signaling Depending on Receptor Context. *PLoS Biol. 4*, e115.
(40) Kamino, M., Kishida, M., Kibe, T., Ikoma, K., Iijima, M., Hirano, H., Tokudome, M., Chen, L., Koriyama, C., Yamada, K., Arita, K., and Kishida, S. (2011) Wnt-5a signaling is correlated with infiltrative activity in human glioma by inducing cellular migration and MMP-2. *Cancer Sci. 102*, 540−548.
(41) Skronska-Wasek, W., Mutze, K., Baarsma, H. A., Bracke, K. R., Alsafadi, H. N., Lehmann, M., Costa, R., Stornaiuolo, M., Novellino, E., Brusselle, G. G., Wagner, D. E., Yildirim, A. Ö., and Königshoff, M. (2017) Reduced Frizzled Receptor 4 Expression Prevents WNT/β-catenin-driven Alveolar Lung Repair in COPD. *Am. J. Respir. Crit. Care Med. 196*, 172.
(42) Saaf, A. M., Halbleib, J. M., Chen, X., Yuen, S. T., Leung, S. Y., Nelson, W. J., and Brown, P. O. (2007) Parallels between Global


DOI: 10.1021/acs.biochem.7b01087
*Biochemistry* 2018, 57, 839−851

Transcriptional Programs of Polarizing Caco-2 Intestinal Epithelial Cells In Vitro and Gene Expression Programs in Normal Colon and Colon Cancer. *Mol. Biol. Cell 18*, 4245−4260.
(43) Galiatsatos, P., and Foulkes, W. D. (2006) Familial Adenomatous Polyposis. *Am. J. Gastroenterol. 101*, 385−398.
(44) Kilander, M. B. C., Petersen, J., Andressen, K. W., Ganji, R. S., Levy, F. O., Schuster, J., Dahl, N., Bryja, V., and Schulte, G. (2014) Disheveled regulates precoupling of heterotrimeric G proteins to Frizzled 6. *FASEB J. 28*, 2293−2305.



DOI: 10.1021/acs.biochem.7b01087
*Biochemistry* 2018, 57, 839−851